

# Heterodyne Laser-Doppler Vibrometer with a Slow-Shear-Mode Bragg Cell for Vibration Measurements up to 1.2 GHz

Christian Rembe, Sebastian Boedecker, Alexander Dräbenstedt, Fred Pudewills, Georg Siegmund  
Research & Development, Polytec GmbH  
Polytec Platz 1-7, 76337 Waldbronn

## ABSTRACT

Several new applications for optical ultra-high frequency (UHF) measurements have been evolved during the last decade by advancements in ultra-sonic filters and actuators as well as by the progress in micro- and nanotechnology. These new applications require new testing methods. Laser-based, non-influencing optical testing is the best choice. In this paper we present a laser-Doppler vibrometer for vibration measurements at frequencies up to 1.2 GHz. The frequency-shifter in the heterodyne interferometer is a slow-shear-mode Bragg cell. The light source in the interferometer is a green DPSS (diode pumped solid state) laser. At this wavelength the highest possible frequency shift between zero and first diffraction order is a few MHz above 300 MHz for a slow shear-mode Bragg cell and, therefore, the highest possible bandwidth of the laser-Doppler vibrometer should usually be around 300 MHz. A new optical arrangement and a novel signal processing of the digitized photo-detector signal is employed to expand the bandwidth to 1.2 GHz. We describe the utilized techniques and present the characterization of the new ultra-high-frequency (UHF) vibrometer. An example measurement on a surface acoustic wave (SAW) resonator oscillating at 262 MHz is also demonstrated. The light-power of the measurement beam can be switched on rapidly by a trigger signal to avoid thermal influences on the sample.

Keywords: Ultra-sonic testing, ultra-high-frequency vibrations, laser-Doppler vibrometry, surface acoustic waves

## 1. INTRODUCTION

Interferometric vibration sensors for high frequencies have been investigated since years for measuring surface acoustic waves [1]. Common conditions for ultrasonic testing are high vibration frequencies from several MHz to the GHz regime and tiny vibration amplitudes of a maximum of a few tens of nanometers. Optical sensors have been developed to enable laser-induced ultra-sonic testing in filthy and loud environments on mechanical specimens with a rough surface. The existing commercial systems have high laser powers of several 100 mW and a rather large measurement spot of a few tens of micrometers. These systems are not suited for the new applications where a tiny measurement spot prohibits a high energy transfer to the specimen [2,3,4,5].

Optical measurements of ultrasonics with microscopic lateral resolution have been demonstrated by several research groups. High vibration frequencies lead to short acoustical wavelengths in dependence on the speed of sound. For example, typical speeds of sound in solids lie between 2000 and 10000 m/s [6] and, therefore, acoustical wave lengths at 1 GHz have values between 2 and 10  $\mu\text{m}$ . Thus, the spot diameter to measure GHz vibrations should be less than 1  $\mu\text{m}$  to make sure that the measurement beam impinges just one equally deflecting point.

An optical lock-in vibration detection using photorefractive frequency domain processing has been presented by the Idaho National Engineering Laboratory [7, 8, 9]. This system can perform a full-field measurement but is limited to measure the response to the driving signal by their lock-in approach. Probably, the most well-known technique is a homodyne Michelson interferometer stabilized on the quadrature point of the interference signal [1, 10, 11, 12]. In this kind of systems the interferometer is locked by a control circuit on the sensitive slope of the interference signal in the middle between a bright and a dark fringe by keeping the optical path length difference of measurement and reference

beams constant. Actually this homodyne technique of laser-vibration measurement has been already introduced in the 1960s [13, 14] and is widely used in research laboratories. However, the homodyne interferometer with quadrature point stabilization is not suitable for a robust industrial sensor, because the reference mirror is positioned with a piezoelectric transducer. In addition, the calibration of the vibration amplitude measurement is not reliable because the interference signal amplitude is dependent on the surface reflectivity and the vibration amplitude. Therefore, we have advanced heterodyne laser-Doppler vibrometry [15, 16] to measure frequencies in the GHz range. Ultrasonic testing with heterodyne interferometers have been demonstrated in the past [17] but, to our knowledge, the highest demonstrated bandwidth so far is 100 MHz [18]. The beat frequency of laser modes of a HeNe laser has been used in [18] to obtain a carrier frequency of 1090 MHz. Thus, the bandwidth in [18] is limited by the demodulator and not by the carrier frequency. However, for this approach the light power is limited to the low power of the laser modes and high power is necessary to obtain high resolution at high bandwidths.

We present a heterodyne laser-Doppler-vibrometer design to measure vibration frequencies up to 1.2 GHz where the laser power can be selected independently on the frequency shift. The laser power of the measurement beam can be dimmed and switched to maximal power in microseconds to impinge only light power to the specimen during data acquisition. This is particularly important for vibration measurements in nanomechanical resonators [19, 20], which seem to be a very interesting application field for our new broad-bandwidth GHz-laser-Doppler vibrometer. Bulk and surface acoustic wave filters, RF-MEMS, ultrasound devices, ultrasound actuators, and laser-induced ultra-sonic testing are other possible applications we have in mind for our sensor.

## 2. THEORETICAL SENSITIVITY AND RESOLUTION LIMITS

An heterodyne laser-Doppler vibrometer consists of a heterodyne interferometer and a demodulator for the phase-modulated carrier. The ultimate limit for the heterodyne vibrometry is the so called frequency modulation (fm) threshold. This limit is reached when the power of heterodyne carrier is equal to the power of the noise in the demodulator bandwidth. The power is proportional to the square of the rms current and, thus,

$$\bar{i}_c^2 > \bar{i}_{noise}^2 \quad (1)$$

with  $\bar{i}_c$  the rms current of the carrier and  $\bar{i}_{noise}$  the rms noise current in the bandwidth  $B$  of the demodulator and/or the detector. The noise of the demodulated signal increases disproportionately if (1) is not hold. Highest resolution can be achieved with a heterodyne vibrometer if the noise is limited by the shot noise of the detected light [21]. Therefore, the detector amplification, which depends on the detector load resistance, has to be low enough so that the light power of the reference beam can be high enough within the dynamic range of the sensitivity. This is necessary to ensure

$$\bar{i}_{sh} > \bar{i}_{th} \quad (2)$$

with  $\bar{i}_{sh}$  the rms shot-noise current and  $\bar{i}_{th}$  the rms noise current of all other noise sources. The heterodyne interferometer is called shot-noise limited if (2) is valid. In practice condition (2) can be checked if the noise level in the spectrum of the detector signal increases by at least 3 dB when the reference light impinges the detector. The first task in the development of a laser-Doppler vibrometer for GHz vibrations is to design a shot-noise limited heterodyne interferometer. The square of the rms noise current results in [21]

$$\bar{i}_{noise}^2 = \bar{i}_{sh}^2 = 2KqB(P_m + P_r) \quad (3)$$

for a shot-noise limited interferometer with  $q = 1.602177 \cdot 10^{-19}$  C the charge of an electron,  $K = \eta q / h \nu$  the conversion parameter of the detector,  $P_m$  the power of the measurement light impinging the detector and  $P_r$  the power

of the reference light. In addition,  $h = 6.6261 \cdot 10^{-34}$  J is the Planck's constant,  $\eta$  is the quantum efficiency of the detector, and  $\nu = c/\lambda$  is the laser-light frequency. The speed of light is  $c = 299792458$  m/s.

The second task that has to be considered is to compute the light power level when the heterodyne interferometer reaches the fm threshold. Therefore, the squared rms carrier current

$$\bar{i}_c^2 = 2K^2 \varepsilon^2 P_m P_r \quad (4)$$

of the detector signal

$$i_s = K \left[ P_m + P_r + 2K \sqrt{P_m + P_r} \cos(\omega_c t - \varphi(t)) \right] \quad (5)$$

has to be higher than the square of the rms noise current. In (4) and (5)  $\varepsilon$  is the heterodyning efficiency, which takes into account any degradation of the photocurrent due to optical distortions or misalignments, and

$$\varphi(t) = \frac{4\pi}{\lambda} s(t) \quad (6)$$

is the time dependent phase modulation by the specimen displacement  $s(t)$ . In (6)  $\lambda$  is the wavelength. The minimum light power to exceed the fm threshold for a given reference power  $P_r$  and bandwidth  $B$  can be derived from (3) and (4)

$$P_m > \frac{2qBK P_r}{2K^2 \varepsilon^2 P_r - 2qBK} \quad (7)$$

For typical values [21]  $\eta = 0.8$  and  $\varepsilon = 0.8$  as well as for the chosen parameters of the heterodyne interferometer (see next section) of  $P_r = 4$  mW and  $B = 2$  GHz the minimum sensitivity the minimum power of measurement light on the detector results in

$$P_m > 1.46 \text{ nW.}$$

High numerical apertures (NA) are necessary to achieve spot diameters of a few  $\mu\text{m}$  or even less than a  $\mu\text{m}$ . Much more returning measurement laser power can be expected because usually good reflecting surfaces are investigated. Assuming a measurement laser power of 2 mW on the detector the expected resolution for these numbers can be computed. Considering the SNR of the detector signal [21]

$$SNR = \frac{\bar{i}_s^2}{\bar{i}_{sh}^2} = \frac{\eta \varepsilon^2 P_m P_r}{h \nu B (P_m + P_r)} \quad (8)$$

the resolution results to

$$\bar{s}_{res} = \frac{\lambda}{\sqrt{8} \pi} \sqrt{\frac{h \nu (P_m + P_r) 1 \text{ Hz}}{\eta \varepsilon^2 P_m P_r}} = 1.4 \text{ fm} \quad (9)$$

in respect to a bandwidth of 1 Hz. Obviously 1 Hz bandwidth can not be realized with a ultra-high-frequency laser-Doppler vibrometer. For example, the Nyquist-Shannon theorem [22] requires at least a sample rate of 2 GSamples/s to acquire a signal with 1 GHz bandwidth. Therefore, a digitalization of 8 bit results in a data rate of 2 Gbyte per second. A typical computation of a fast Fourier transform (FFT) spectrum [21] with 12800 FFT lines requires 25600 time samples. This is just a duration of 12.8  $\mu$ s for data acquisition and results in a frequency resolution of approximately  $B_{FFT} = 78$  kHz. This corresponds to the resolution bandwidth of the vibration amplitude measurement with the heterodyne interferometer. Thus, a realistic vibration-amplitude resolution that can be expected with an ultra-high-frequency vibrometer in an FFT-vibration spectrum is

$$\bar{s}_{res} = \bar{s}'_{res} \sqrt{B_{FFT}} = 391 \text{ fm} \quad . \quad (10)$$

A further improvement of resolution can be obtained for stationary signals utilizing averaging techniques.

### 3. OPTICAL SETUP

The optical part of the laser-Doppler vibrometer is the heterodyne interferometer. A large frequency shift between reference and measurement beam is essential to provide the bandwidth necessary for the phase modulation by specimen vibration. Vibration amplitudes  $s_0$  in the range between 10 MHz and 1 GHz can be expected not to exceed a few nanometers  $s_0 \ll \lambda/4$ . It can be assumed that the detector signal (5) can be approximated by [21]

$$\begin{aligned} i_s &= K \left[ P_m + P_r + 2K \sqrt{P_m + P_r} \cos(\omega_c t - M \cos(\Omega t)) \right] \\ &\approx K \left[ P_m + P_r + 2K \sqrt{P_m + P_r} \left( \cos(\omega_c t) + \frac{M}{2} \cos(\omega_c t + \Omega t) - \frac{M}{2} \cos(\omega_c t - \Omega t) \right) \right] \end{aligned} \quad (11)$$

using the Bessel-function extension of the phase-modulated carrier with the tiny modulation index  $M = 4\pi s_0/\lambda \ll 1$ . Therefore, for a standard demodulator the carrier frequency has to be larger than the vibration frequency  $\omega_c > \Omega$  to ensure that negative frequencies in (11) are avoided. To provide a maximum vibration measurement bandwidth a maximal carrier frequency should be provided. There are several options to generate a frequency shift between two laser beams. The first possibility is to use 2 laser modes of a stabilized laser [18]. This option has the disadvantage that the laser source with its properties is fixed. For example, the system described in [18] uses a stabilized HeNe and, therefore, the total laser power of reference and measurement beam is below 1 mW. The second possibility are two phase-locked laser sources [23]. These systems are very complex and are only suited for laboratory setups. It is not a technique suited for a commercial system yet. The third option is the use of nonlinear multi-photon processes [24] which are not efficient enough for a commercial heterodyne interferometer. The last option is an acousto-optic frequency shifter, a Bragg cell. Bragg cells for high frequency shifts ( $> 500$  MHz) between zero and first diffraction order are not efficient (less than 1 %). Therefore, a slow-shear mode cell [25] should be used. The most efficient bragg-cell material in the visible region is TeO<sub>2</sub>. It provides efficiencies of over 90%. But the maximum shift of a TeO<sub>2</sub>-Bragg cell in the visible region is below 350 MHz. Higher shifts can only be achieved with higher diffraction orders and special Bragg-cell designs. As interferometer setup we chose the Mach-Zehnder arrangement. The schematic of our heterodyne interferometer can be seen in figure 1.

As mentioned above, high-frequency measurements with high bandwidth require relatively high laser intensity and, of course, an commercial measurement sensor should be equipped with a cost efficient laser. We have chosen a compact green diode-pumped, solid-state (DPSS) laser with frequency-doubled light from a NdYAG-crystal. The laser light has low amplitude noise and a pure Gaussian beam profile. The  $M^2$ -value is less than 1.1. Therefore we can focus the laser beam to a diffraction limited spot of less than 1  $\mu$ m using an high NA microscope objective. We employ the setup of a confocal laser-Doppler vibrometer microscope [26] to achieve highest lateral resolution. The measurement beam is circular polarized which additionally reduces the laser spot diameter [27]. The line width of the laser is 5 MHz but since

the specimen is always in the focus of a microscope objective we have designed an equal path-length interferometer. The heterodyne interferometer signal is detected with a fast PIN photo diode (2 GHz bandwidth) and is captured and saved with a fast digital oscilloscope. We have chosen 2 GHz bandwidth for the detector to measure with three times the bandwidth of the carrier frequency. This allows us to employ a novel bandwidth-extension algorithm described in section 6. The 5 mW measurement beam is focussed to an area of less than  $1 \mu\text{m}^2$ . This corresponds to an area power density of more than  $5 \text{ GW}/\text{m}^2$ . The demolition of the sample has to be avoided and thermal influences should be minimized. Therefore, the sensor head can be triggered to illuminate the sample only during the rather short measurement time.

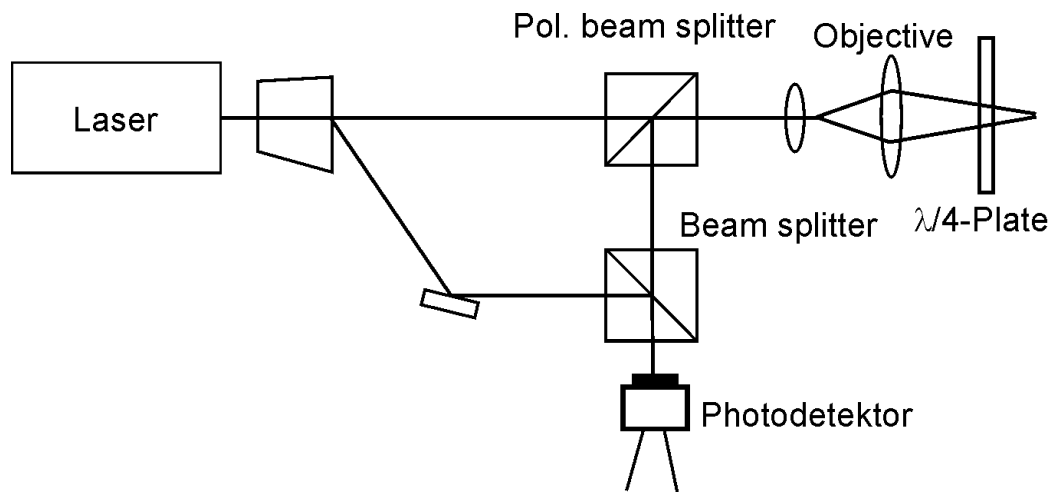


Figure 1: Schematic of the heterodyne interferometer.

#### 4. DATA-ACQUISITION AND DEMODULATION SYSTEM

The photo-detector bandwidth is 2 GHz and with the extended bandwidth algorithm described in section 6 all information in this bandwidth should be used for evaluation. Analog decoders with this bandwidth have their own frequency response. Calibrated generators for fm-modulated signals with a modulation bandwidth of several 100 MHz are not available. It is impossible to calibrate such demodulators because there are no test signals. Therefore, we have chosen to demodulate the carrier signal from the photodetector digitally because modern oscilloscopes with high-frequency bandwidth are available and can be used as fast digitizers. No unknown response behaviour or thermal influences are present after the signal is digitized. The transfer function of our photo detector is calibrated with a modulated laser diode and the cables between detector and oscilloscope can be characterized with a network analyzer. Therefore, any component in the signal processing chain can be calibrated. The sample rate for the detector signal should be at least twice the detector bandwidth to avoid aliasing effects. Thus, the oscilloscope has to provide a minimum sample rate of 4 GSamples per second. The oscilloscope has a dynamic of 8 bit and, therefore, acquires the data at a minimum rate of 4 Gbyte per second. Actually, there are no bus systems or real-time processing units to perform the demodulation in real time. Thus, the data is sampled and stored in the memory of the oscilloscope. The digitized detector signal is transferred from the oscilloscope to a PC after the measurement and an off-line demodulation is performed. The maximum measurement duration and the resulting frequency resolution depend on the sample rate and the size of the memory in the oscilloscope. The whole measurement procedure has to be synchronized accurately with the investigated event. The measurement signal is stored and evaluated later on. The setup of our data-acquisition and demodulation system is shown in figure 2.

The user can arrange the measurement from the personal computer (PC). The measurement is synchronized by a function generator which generates the driving signal for the sample, the trigger signal for the data acquisition with the oscilloscope, and the trigger signal to turn on the measurement light to full power. The junction box includes the driver

for the Bragg cell and delivers the heterodyne carrier frequency as stored number to the PC. The software in the PC demodulates the detector signal by the arctan method [21]. The signal processing scheme of the arctan method is shown in figure 3.

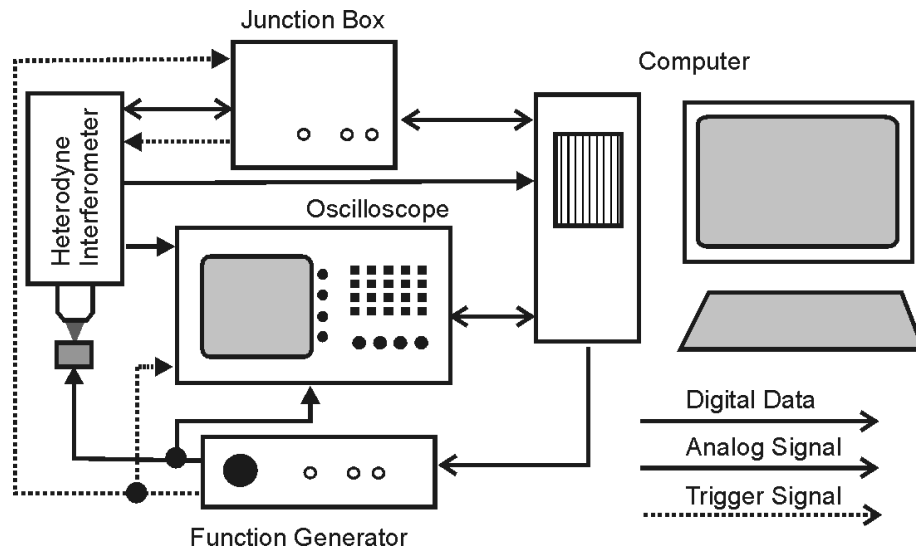


Figure 2: Schematic of the ultra-high-frequency, laser-Doppler vibrometer with heterodyne interferometer, junction box, oscilloscope for data acquisition, function generator and personal computer.

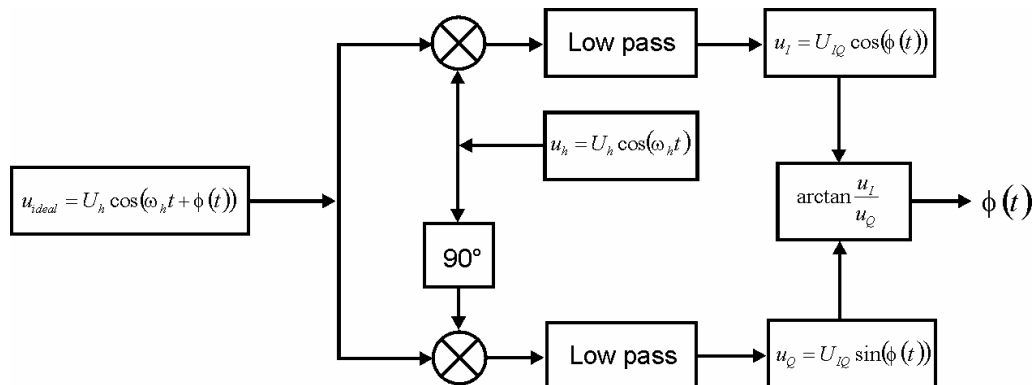


Figure 3: Signal processing scheme of the arctan-demodulation method.

## 5. EXPERIMENTS

The noise level of the detector signal has to increase at least about 3 dB if light impinges the detector for a shot-noise limited system as mentioned in section 2. Figure 4a demonstrates the spectral noise distribution of the detector signal if no light impinges the detector for a resolution bandwidth of 3 kHz and figure 4b demonstrates the noise level when 4 mW light power impinge the detector. The noise level increases 3 dB and, thus, the heterodyne interferometer is shot-noise limited with 4 mW laser power. The difference between carrier strength and detector noise shows if the system is aligned properly and if a high value for the heterodyning efficiency is achieved. Figure 5 demonstrates the spectrum of the detector signal in the heterodyne interferometer if the measurement beam impinges a mirror. The sensitivity of our photo diode at 532 nm is  $K = 0.25$  A/W and the conversion gain of our transimpedance amplifier is  $G_T = 500$  V/A. Thus, the expected carrier strength for 2 mW reference light power and 2 mW measurement light power results with

equation (5) in 2dBm. The noise level follows from (3) to  $P_{noise} = 10 \log(G_T^2 2KqB(P_r + P_m)/10^{-3}) = -113$  dBm for 3 kHz resolution bandwidth (RBW) and corresponds well with the measurement in figure 4.

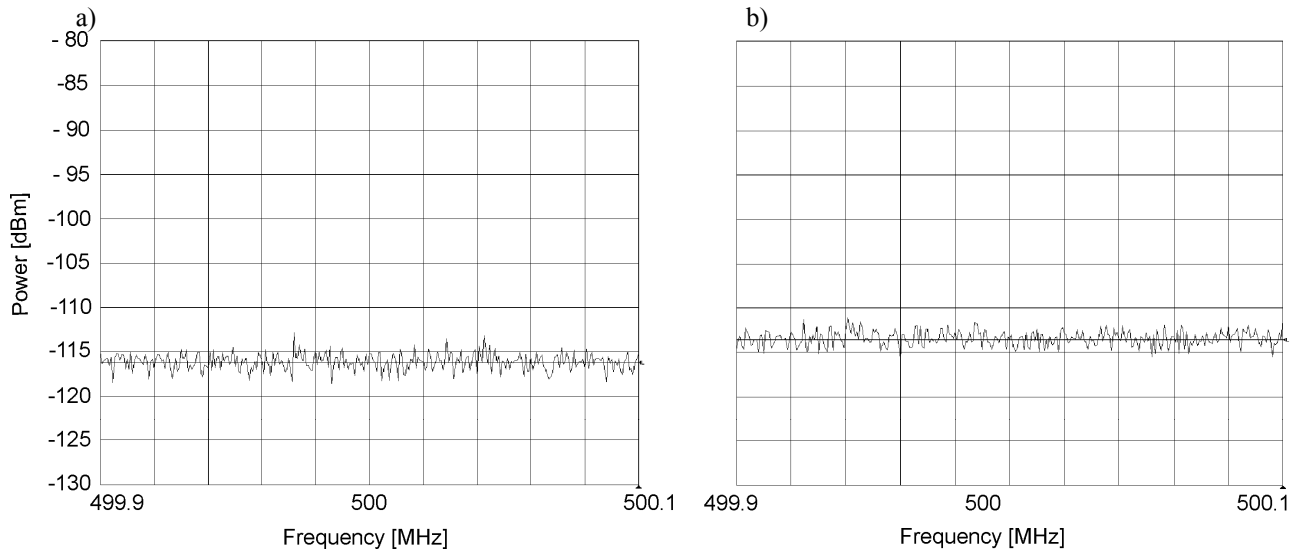


Figure 4: Noise-level in the spectrum of the detector signal if no light impinges the detector (a) and noise-level in the spectrum of the detector signal if 4 mW light power impinges the detector (b). The RBW is 3 kHz.

The measurement in figure 5 with 2 mW reference power and 2 mW power of the returning measurement light demonstrates that the beams are efficiently interfered and detected because the carrier has a power of 0 dBm. Just 2 dB are missing in respect to the theoretical value.

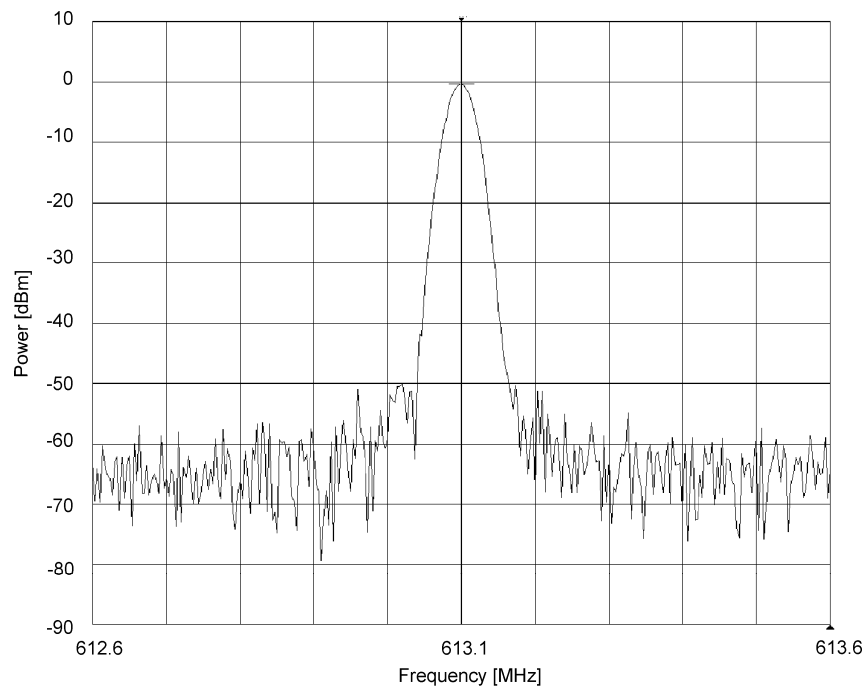


Figure 5: Signal carrier in the noise spectrum of the photo-detector signal measured on a mirror. The RBW is 30 kHz and the carrier strength is 0 dBm for 2 mW reference and 2 mW measurement light.

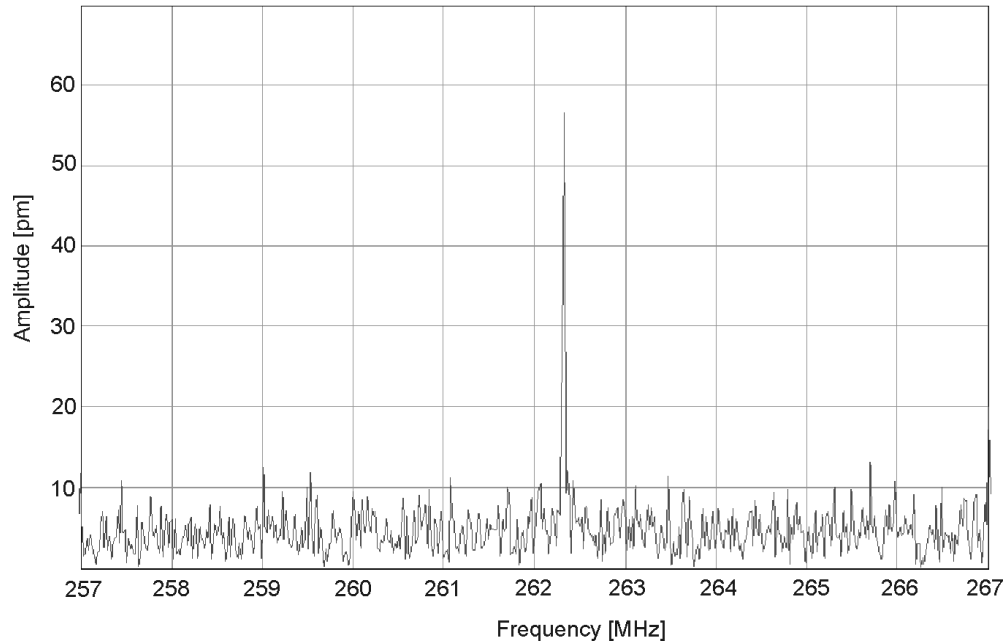


Figure 6: FFT spectrum of the digital demodulated displacement signal of the heterodyne interferometer. The 56 pm vibration amplitude of a SAW-device oscillating at 262.3 MHz can be measured accurately. The RBW is 19 kHz.

Figure 6 shows the FFT spectrum of a measurement on an surface-acoustic-wave (SAW) resonator oscillating at 262 MHz with an amplitude of 56 pm. A measurement duration of 51.2  $\mu\text{s}$  at a sample rate of 5 GSample/s results in a 256000 data points. Thus, the resolution bandwidth of this measurement is 19.5 kHz and the noise level is at 30  $\text{fm}/\sqrt{\text{Hz}}$ . We use an oscilloscope with 25 Mbyte memory for the acquired signal and can realize 5 ms measurement time and, therefore, a frequency resolution of 200 Hz. Our system can detect amplitudes below 1 pm at frequencies of hundreds of MHz with a broad-bandwidth measurement. Consequently it is possible to investigate vibrations at these high frequencies with broad-bandwidth excitations, e.g. periodic chirp signals [21].

## 6. BANDWIDTH EXTENSION ALGORITHM

High frequencies in the hundreds of MHz range correspond to vibrations with maximal amplitudes of a few nanometers. Therefore, the phase-modulated carrier signal contains only the lowest order of Bessel lines as it is demonstrated with equation (11). It is also demonstrated with equation 11 that the  $-1$  order and  $+1$  order Bessel lines have a well-determined phase relation. This fact has enabled us to realize an algorithm to extend the measurement bandwidth by a factor of 2. The algorithm takes only the frequency components of the detector signal into account which are higher than the carrier frequency and constructs a new carrier signal at twice the carrier frequency. In the following the new carrier frequency is called extended carrier frequency. The frequency components at lower frequencies in respect to the extended carrier frequency are computed from the frequency components higher than the extended carrier. Then simple digital down-mixing and arc-tangent demodulation can be performed to obtain a displacement signal with twice the possible bandwidth. Since we have not organized a sample so far capable of oscillating at 1.2 GHz we show a simulation of the demodulation of the 1.2 GHz vibration with 5 nm amplitude in figure 7a.

The detector signal generated by the beat of the modulated measurement beam and reference beam can be simulated with equation 11. The spectral power density spectrum can be computed from the simulated detector signal. The result is shown in figure 7b and it is demonstrated that the  $-1$  order Bessel line is shifted close to the 0 order Bessel line which corresponds to the carrier frequency. It is obvious that the 0-order and the  $+1$  order of the Bessel lines contain all information of phase and amplitude. The time signal of the detector signal is stored and transferred to the PC. In the PC

the length of the detector signal measurement is adjusted to consider a total measurement duration  $T_{total} = n/f_c$  with  $n$  an integer. Therefore, the carrier frequency is represented by one discrete Fourier transform (DFT) line. Our algorithm computes a new DFT-spectrum with twice the carrier frequency. The carrier-frequency amplitude and all amplitudes of frequency components higher as the carrier are shifted by the value of the index of the carrier frequency  $i_c$  to higher frequency components.

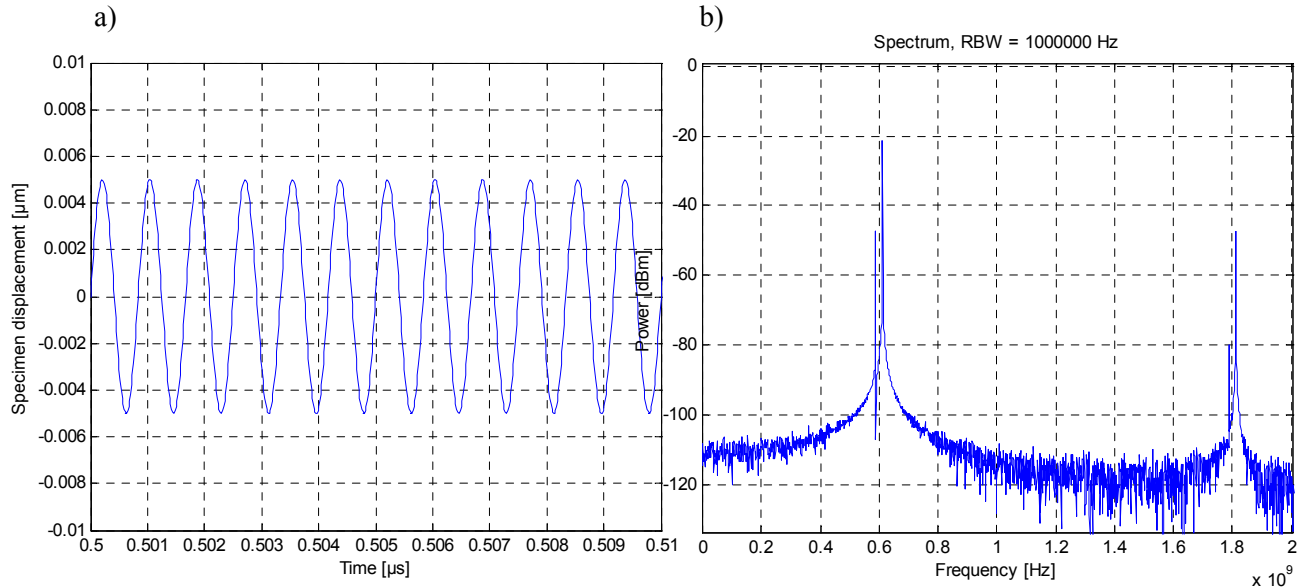


Figure 7: Simulated specimen displacement of a 1.2 GHz vibration with 5 nm amplitude (a) and simulated power density spectrum of the detector signal (b).

Thus a new extended spectrum is generated containing  $i_c$  more frequency components. The amplitudes in the extended spectrum at frequencies smaller the extended carrier frequency are constructed by the components higher than the extended carrier frequency. The fixed phase relation between the +1 and -1 order Bessel lines demonstrated by equation 11 is considered in this computation. In the complex spectrum the -1 order Bessel line is the negative complex conjugate of the +1 order Bessel line. After the construction of the extended spectrum the extended detector signal is generated by the inverse DFT. This extended signal is demodulated by the arctan method, demonstrated in figure 3 with a computed reference signal twice the frequency of the optical heterodyne carrier. The demodulated signal in figure 8 corresponds well with the simulated displacement shown in figure 7a that has been used to compute a detector signal with a 1.2 GHz modulation. The spectrum of the modulated carrier signal is shown in figure 7b.

We have also investigated motions containing several frequency components. The signal is determined with high accuracy even if higher harmonics of the basis frequency component are present in the specimen motion. In this case the second order Bessel line of the basis vibration frequency component is at the same frequency as the first order Bessel line of the first harmonics of the basis vibration frequency. The extended-bandwidth technique presented in this paper is well-suited to investigate high-frequency vibrations with broad-bandwidth excitation signals, e.g with a periodic chirp excitation. The bandwidth extension can be used to study non-harmonic and even single transient processes for displacement amplitudes of a few nanometers. Figure 9a) demonstrates the simulation of a vibration containing 100 MHz, 200 MHz, ... , 1 GHz frequency components and figure 9b) shows the demodulated displacement signal using the bandwidth extension algorithm. The non-harmonic motion is demodulated accurately for small displacement amplitudes.

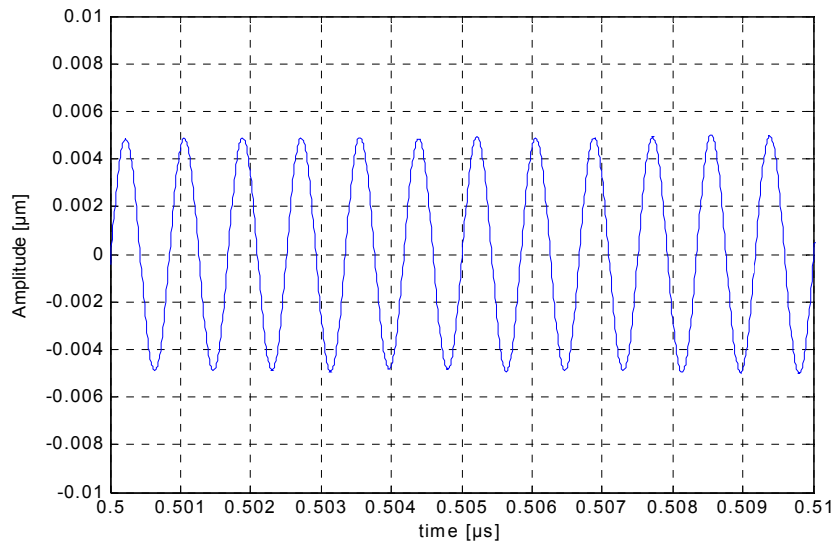


Figure 8: Simulation of a demodulated carrier, the modulation frequency is 1.2 GHz. Note that the amplitude of 5 nm is demodulated correctly.

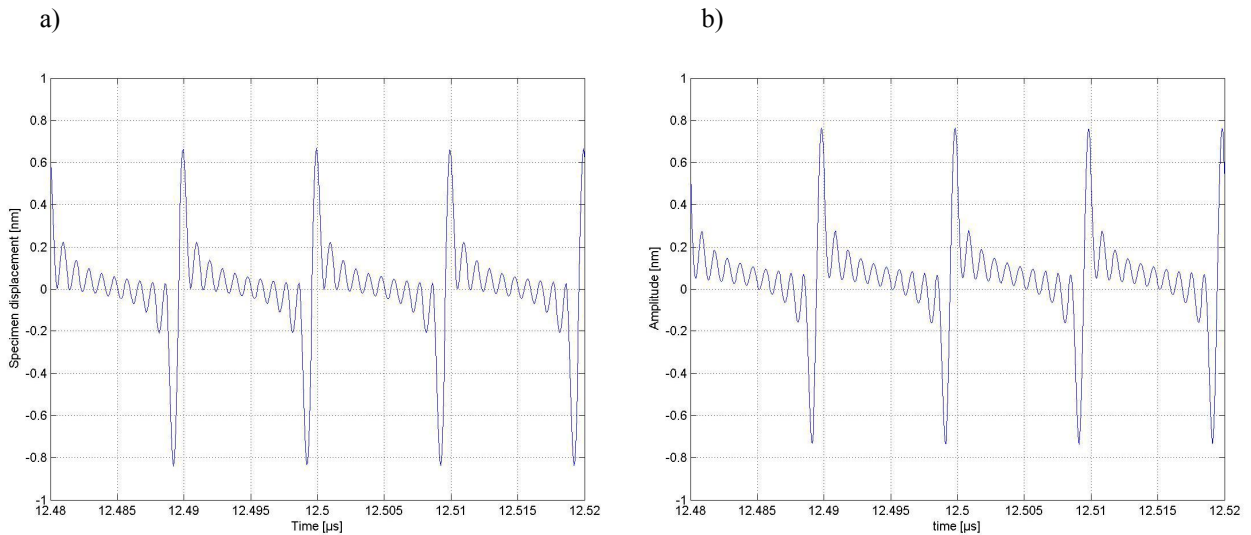


Figure 9: Simulation of a non-harmonic specimen displacement (a) and displacement signal obtained with the bandwidth extension algorithm.

## 7. CONCLUSIONS

We have developed a novel laser-Doppler vibrometer for broad bandwidth measurements at vibration frequencies up to 1.2 GHz. Our heterodyne interferometer utilizes a special Bragg cell to obtain a frequency shift of 613 MHz between reference and measurement beam. The detector signal is digitized by using a fast digital oscilloscope as data acquisition unit. The digital detector signal is demodulated by the arctan method. The amplitude resolution of our system is in the sub-pm range. The capabilities of our new system have been demonstrated by the measurement of a vibration in a SAW resonator. We measured a 56 pm vibration amplitude at a frequency of 262 MHz. We have demonstrated a novel

bandwidth extension algorithm to measure vibrations with nanometer amplitudes with up to twice the frequencies of the heterodyne carrier. Broadband excitation can be employed and non-harmonic vibrations can be investigated.

Bulk and surface acoustic wave filters, RF-MEMS, ultrasound devices, ultrasound actuators, and laser-induced ultrasonic testing are the applications for the ultra-high-frequency vibrometer. A very interesting application is the investigation of vibrations in nanobeams as they have been explored by Eshashi et al. [28, 29] at low frequencies up to a few 100 kHz. Our new patent-pending system may support to explore the new boundaries at higher frequencies described theoretically in [20].

## ACKNOWLEDGEMENT

The project has been funded by the Bundesministerium für Bildung und Forschung (BMBF Förderkennzeichen 16SV1934).

## REFERENCES

- [1] J.W. Wagner, Optical Detection of Ultrasound, in Physical Acoustics Vol. XIX, W.P. Mason Ed (Academic Press, 1999), 201-266
- [2] P. Delaye, S. de Rossi, G. Roosen, Photorefractive vibrometer for detection of high-amplitude vibrations on rough surfaces, *J. Opt. A: Pure Appl. Opt.* Vol. 2 (2000), 209-215.
- [3] D.M. Pepper, D.A. Rockwell, G.J. Dunning, Nonlinear Optical Phase Conjugation, *IEEE Circuits & Devices*, September 1991, 21-34.
- [4] D.M. Pepper, Optics in Factory, *Optics & Photonics News*, May 1997, 33-40.
- [5] M.B. Klein, G.J. Dunning, P.V. Mitchell, T.R. O'Meara, M. Chiao, Y. Owechko, D.M. Pepper, High-Volume Industrial Applications of Remote Laser-Based Ultrasound for Weld-Joint Inspection, *Proc. ICALEO*, San Diego, CA, November, 1995.
- [6] H. Kuchling, *Taschenbuch der Physik*, Fachbuchverlag Leibzig-Köln, 15. Auflage, 1995, 641.
- [7] T.C. Hale, K.L. Telschow, Optical Lock-in Vibration Detection using photorefractive Frequency Domain Processing, *Appl. Phys. Lett.*, Vol. 69, 1996, 2632-2634.
- [8] K.L. Telschow, V.A. Deason, Imaging Laser Ultrasonics Measurement of the Elastodynamic Properties of Paper, *IEEE Ultrasonics Symposium*, Atlanta, October 7-10, 2001.
- [9] K.L. Telschow, V.A. Deason, D.L. Cottle, Full-Field Imaging of Acoustic Motion at Nanosecond Time and Micron Length Scales, *IEEE Ultrasonics Symposium*, Munich, October 8-11, 2002.
- [10] J.E. Graebner, Optical Scanning Interferometer for Dynamic Imaging of High-Frequency Surface Motion, *IEEE Ultrasonics Symposium*, Puerto Rico, October 22-25, 2001.
- [11] J.E. Graebner, Optical Mapping of Surface Vibrations on a Thin-Film Resonator near 2 GHz, *Puerto Rico*, October 22-25, 2001.
- [12] J.V. Knuutila, P.T. Tikka, M.M. Salomaa, Scanning Michelson Interferometer for Imaging Surface Acoustic Wave Fields, *Opt. Lett.*, Vol. 25, 2001, 613-615.
- [13] H.A. Deferrari, F.A. Andrews, Laser-Interferometric Technique for Measuring Small-Order Vibration Displacements, *J. Acoust. Soc. Am.*, Vol. 39, 1966, 979-980.
- [14] H.A. Deferrari, R.A. Darby, F.A. Andrews, Vibrational Displacement and Mode-Shape Measurement by a Laser Interferometer, *J. Acoust. Soc. Am.*, Vol. 42, 1967, 982-990.
- [15] G.A. Massey, An Optical Heterodyne Ultrasonic Image Converter, *Proc. of the IEEE*, Vol. 56, 1968, 2157-2161.
- [16] F.J. Eberhardt, F.A. Andrews, Laser Heterodyne System for Vibration Measurement and Analysis, *J. Acoust. Soc. Am.*, Vol. 48, 1970, 603-609.
- [17] J. Huang, J.D. Achenbach, Dual-Probe Laser Interferometer, *J. Acoust. Soc. Am.*, Vol. 90, 1991, 1269-1274.
- [18] H. Kawakatsu, S. Kawai, D. Saya, M. Nagashio, D. Kobayashi, H. Toshiyoshi, H. Fujita, Towards Atomic Force Microscopy up to 100 MHz, *Rev. Sci. Instrum.* Vol. 73, 2002, 2317-2320.
- [19] K.L. Ekinci, M.L. Roukes, Nanoelectromechanical Systems, *Rev. Sci. Instrum.*, Vol. 76, 061101 (2005).
- [20] I. Katz, A. Retzker, R. Straub, R. Lifshitz, Signatures for a Classical to Quantum Transition of a Driven Nonlinear Nanomechanical Resonator, *Phys. Rev. Lett.*, PRL 99, 040404 (2007).
- [21] C. Rembe, G. Siegmund, H. Steger, M. Wörtge, "Measuring MEMS in Motion by Laser-Doppler Vibrometry", in *Optical Inspection of Microsystems*, Optical Science and Engineering Series Vol. 109, edited by Wolfgang Osten, (Boca Raton, Taylor and Francis Books, ISBN 0849336821, 2006), pp. 245-292.
- [22] C.E. Shannon, Communication in the presence of noise, *Proc. of the IRE*, Vol. 37, 1949, 10-21.
- [23] H.R. Telle, H. Li, Phase-Locking of Laser Diodes, *Electron. Lett.*, Vol. 26, 1990, 858-859.
- [24] W. Demtröder, *Laser Spectroscopy*, Third Edition, Springer Verlag, Berlin, 2003.

- [25] J. Xu, R. Stroud, *Acousto-Optic Devices*, Wiley Series in Pure and Applied Optics, Ed. J. W. Goodman, John Wiley & Sons, New York, 1992.
- [26] C. Rembe, A. Dräbenstedt, "Laser-scanning confocal vibrometer microscope: Theory and experiments", *Rev. Sci. Instrum.* Vol. 77, 083702 (2006.)
- [27] R. Dorn, S. Quabis, and G. Leuchs, *Phys. Rev. Lett.* Vol. 91, 232901, 2003.
- [28] T. Ono, M. Esashi, Mass sensing with ultra-thin silicon beams detected by a double-beam laser Doppler vibrometer, *Meas. Sci. Technol.*, Vol 15, 2004, 1977-1981.
- [29] T. Ono, M. Esashi, Stress-induced mass detection with a micromechanical/nanomechanical silicon resonator, *Rev. Sci. Instrum.*, Vol 76, 093107, 2005.